p53 SUMOylation promotes its nuclear export by facilitating its release from the nuclear export receptor CRM1

Aleixo Santiago[a,*], Dawei Li[a,b], Lisa Y. Zhao[a,†], Adam Godsey[a], and Daiqing Liao[a]
[a]Department of Anatomy and Cell Biology, UF Health Cancer Center, and UF Genetics Institute, University of Florida College of Medicine, Gainesville, FL 32610; [b]Department of Urology, Qilu Hospital, Shandong University, Jinan 250012, Shandong, China

ABSTRACT **Chromosomal region maintenance 1 (CRM1) mediates p53 nuclear export. Although p53 SUMOylation promotes its nuclear export, the underlying mechanism is unclear. Here we show that tethering of a small, ubiquitin-like modifier (SUMO) moiety to p53 markedly increases its cytoplasmic localization. SUMO attachment to p53 does not affect its oligomerization, suggesting that subunit dissociation required for exposing p53's nuclear export signal (NES) is unnecessary for p53 nuclear export. Surprisingly, SUMO-mediated p53 nuclear export depends on the SUMO-interacting motif (SIM)-binding pocket of SUMO-1. The CRM1 C-terminal domain lacking the NES-binding groove interacts with tetrameric p53, and the proper folding of the p53 core domain, rather than the presence of the N- or C-terminal tails, appears to be important for p53–CRM1 interaction. The CRM1 Huntington, EF3, a subunit of PP2A, and TOR1 9 (HEAT9) loop, which regulates GTP-binding nuclear protein Ran binding and cargo release, contains a prototypical SIM. Remarkably, disruption of this SIM in conjunction with a mutated SIM-binding groove of SUMO-1 markedly enhances the binding of CRM1 to p53-SUMO-1 and their accumulation in the nuclear pore complexes (NPCs), as well as their persistent association in the cytoplasm. We propose that SUMOylation of a CRM1 cargo such as p53 at the NPCs unlocks the HEAT9 loop of CRM1 to facilitate the disassembly of the transporting complex and cargo release to the cytoplasm.**

Monitoring Editor
A. Gregory Matera
University of North Carolina

Received: Oct 31, 2012
Revised: Jun 24, 2013
Accepted: Jun 24, 2013

INTRODUCTION

Chromosomal region maintenance 1 (CRM1; also known as exportin-1) is a major nuclear export receptor that traffics diverse cargoes, including proteins, small nuclear RNAs, and ribosomal subunits, to the cytoplasm (Fornerod *et al.*, 1997; Hutten and Kehlenbach, 2007; Guttler and Gorlich, 2011). It is a member of the karyopherin-β family of transporter proteins, which mediate the nuclear import and export of various cargoes, including proteins and nucleic acids (Cook and Conti, 2010). CRM1 and other exportins load their cargoes on the binding of GTP-binding nuclear protein Ran (RanGTP) in the nucleus. The cooperative binding kinetics of a cargo and RanGTP to an exportin dramatically increases their affinity to each other (Paraskeva *et al.*, 1999). The ternary cargo-exportin-RanGTP complexes traverse the nuclear pore complex (NPC), where GTP hydrolysis, promoted by RanGTPase-activating protein (RanGAP), leads to the disassembly of the export complex and the release of cargoes to the cytoplasm (Bischoff *et al.*, 1994; Guttler and Gorlich, 2011). RanGAP1 acts exclusively in the cytoplasm (Bischoff *et al.*, 1994) and is constitutively modified with small, ubiquitin-like modifier 1 (SUMO-1; Matunis *et al.*, 1996, 1998; Mahajan *et al.*, 1997). The RanGAP1*SUMO-1 conjugate stably associates with Ubc9, the E2-conjugating enzyme of SUMOylation, and Ran-binding protein 2 (RanBP2)/Nup358, the major component of the cytoplasmic

This article was published online ahead of print in MBoC in Press (http://www.molbiolcell.org/cgi/doi/10.1091/mbc.E12-10-0771) on July 3, 2013.

Present addresses: *Regeneron Pharmaceuticals, Rensselaer, NY 12144; †Department of Medicine, University of Florida, Gainesville, FL 32610.
Address correspondence to: Daiqing Liao (dliao@ufl.edu).

Abbreviations used: CRM1, chromosomal region maintenance 1; FKBP, 12-kDa FK506-binding protein; FRB, FKBP12 and rapamycin-binding domain in the mTOR kinase; HEAT, Huntington, EF3, a subunit of PP2A, and TOR1; NES, nuclear export signal; NPC, nuclear pore complex; PBS, phosphate-buffered saline; PCNA, proliferating cell nuclear antigen; RanBD, Ran-binding domain; RanBP2, Ran-binding protein 2; RanGAP1, Ran GTPase-activating protein 1; RanGTP, GTP-binding nuclear protein Ran; Rev, regulator of expression of viral proteins; SD, yeast selective dropout medium; shRNA, short hairpin RNA; SIM, SUMO-interacting motif; SPN1, snurportin 1; SUMO, small ubiquitin-like modifier.

filaments of the NPC (Mahajan *et al.*, 1997; Saitoh *et al.*, 1997; Matunis *et al.*, 1998). This highly stable ternary complex functions as a multisubunit E3 SUMOylation ligase (Werner *et al.*, 2012). Although substrates of this SUMO ligase have been identified (Dawlaty *et al.*, 2008; Klein *et al.*, 2009; Werner *et al.*, 2012), the role of substrate SUMOylation in the nuclear export mechanism is unclear. RanGAP1 alone cannot activate GTP hydrolysis. It cooperates with RanBP1 or RanBP2 to activate the GTPase in the RanGTP-containing complexes (Guttler and Gorlich, 2011, and references therein). Thus it is possible that the stable SUMO E3 ligase consisting of RanBP2, RanGAP1*SUMO-1, and Ubc9 may couple substrate SUMOylation and GTP hydrolysis for cargo release from CRM1 on the cytoplasmic side of the NPC.

The 21 tandem Huntington, EF3, a subunit of PP2A, and TOR1 (HEAT) repeats of CRM1, each of which consists of an inner and an outer α-helix interconnected by a loop, form a toroid-shaped structure. RanGTP occupies the inner surface of the CRM1 ring, which is not accessible for interacting with cargoes (Dong *et al.*, 2009; Monecke *et al.*, 2009). Therefore a cargo docks to the outer convex surface of the CRM1 toroid structure (Dong *et al.*, 2009; Monecke *et al.*, 2009). This binding mode has been suggested to allow CRM1 to recruit different cargoes that vary greatly in size and shape (Guttler and Gorlich, 2011). Many CRM1 cargoes, including cAMP-dependent protein kinase inhibitor alpha (Wen *et al.*, 1995), the HIV-1 regulator of expression of viral proteins (Rev; Fischer *et al.*, 1995), and p53 (Stommel *et al.*, 1999; Zhang and Xiong, 2001) contain a nuclear export signal (NES) that is rich in leucine residues, which is recognized by the hydrophobic interface between HEAT repeats 11 and 12 on the outer surface of the CRM1 toroid (Dong *et al.*, 2009; Monecke *et al.*, 2009; Guttler and Gorlich, 2011). Despite the specific interaction between an NES short peptide and CRM1, it contributes only a small part to the overall stability of the cargo-CRM1-RanGTP ternary complex. The acidic residues on the convex surface of CRM1 adjacent to the hydrophobic NES-binding groove interact with basic patches on the surfaces of CRM1 cargoes such as snurportin 1 (SPN1) and HIV-1 Rev (Askjaer *et al.*, 1998; Dong *et al.*, 2009). In fact, full-length Rev displays about 100-fold higher affinity to CRM1 than the Rev NES peptide alone (Paraskeva *et al.*, 1999).

Among the loops connecting the inner and outer helices of each HEAT repeat in CRM1, the HEAT9 loop is the longest, with 24 residues. This loop is highly conserved through evolution and notably enriched with hydrophobic and acidic residues, accounting for ~40 and 30% of the total residues, respectively. They form a β-hairpin structure, which extends through the entire central "hole" of the CRM1 toroid and touches the inner helices of HEAT repeats 12–15 (Dong *et al.*, 2009; Monecke *et al.*, 2009). In the structure of RanGTP-CRM1-SNP1 ternary complex, the HEAT9 loop locks RanGTP in one side of the CRM1 central "hole" near the N- and C-terminal HEAT repeats and makes extensive contacts with RanGTP (Dong *et al.*, 2009; Monecke *et al.*, 2009). Additional structural studies suggest that on the association of the Ran-binding domain (RanBD) of RanBP1 with the cargo-CRM1-RanGTP complex, the HEAT9 loop appears to undergo a large movement, reaching closely behind the NES-binding cleft of CRM1, resulting in the closure of the hydrophobic cleft and facilitating cargo unloading from CRM1 (Koyama and Matsuura, 2010). Thus RanBP1 appears to actively displace cargo from CRM1 in the cytoplasm. Similarly, any one of the four RanBDs of RanBP2 could also promote the release of NES-containing cargo from CRM1 (Koyama and Matsuura, 2010). It has been suggested that RanGAP might have an active role in breaking the RanGTP–CRM1 contacts (Guttler and Gorlich, 2011), perhaps in concert with RanBD. On its release from CRM1, RanGTP is readily converted to RanGDP by soluble cytoplasmic or RanBP2-associated RanGAP. Because RanBP2 constitutively associates with RanGAP1*SUMO-1 and Ubc9 and this stable ternary complex possesses E3 SUMO ligase activity (Werner *et al.*, 2012), a potential functional connection between SUMOylation, disassembly of the cargo-CRM1-RanGTP complex, and cargo unloading could be envisioned, given that the HEAT9 loop of CRM1 contains a putative SUMO-interacting motif (SIM; Makhnevych *et al.*, 2009).

The tumor suppressor p53 undergoes active nuclear export. It contains a leucine-rich NES within the tetramerization domain (Stommel *et al.*, 1999). This motif is normally buried in the subunit interfaces of the tetrameric form of p53, and subunit dissociation would be required to reveal this NES for nuclear export. This scenario may indeed exist, as the levels of monomeric p53 seem to increase on its ubiquitination (Carter *et al.*, 2007). The p53 N-terminal transactivation domain appears to contain another NES, and DNA-damage-induced phosphorylation within this motif prevents p53 nuclear export, leading to its nuclear accumulation (Zhang and Xiong, 2001). p53 undergoes SUMOylation at Lys386 with SUMO-1, -2, or -3 (Gostissa *et al.*, 1999; Rodriguez *et al.*, 1999; Kahyo *et al.*, 2001; Chen and Chen, 2003; Stindt *et al.*, 2011), and such modifications actively promote p53 nuclear export (Carter *et al.*, 2007; Heo *et al.*, 2011). Precisely how p53 SUMOylation influences its nuclear export, however, is unknown. Here we report that p53 SUMOylation seems to play a regulatory role in its interaction with CRM1. Whereas SUMOylation of p53 markedly increases its nuclear export, the availability of the SIM-binding groove of the SUMO moiety that is attached to p53 is critical for its nuclear export. We find that the disruption of the hydrophobic SIM-binding cleft of SUMO-1 attached to p53 greatly stabilizes the binding of p53-SUMO-1 to the CRM1 V430K mutant, in which the putative SIM in the HEAT9 loop is mutated. Our results suggest that cargo SUMOylation appears to play an important role in facilitating cargo release from CRM1 during nuclear export.

RESULTS

p53 SUMOylation attenuates p53 transactivation activity

Because the SUMO moiety is quickly removed from SUMO-conjugated substrates in cells, we used two approaches to model the effect of p53 SUMOylation on its function. We fused SUMO in-frame to the C-terminus of p53 to generate a p53-SUMO construct. We also used rapamycin-induced heterodimerization to chemically attach a SUMO moiety to the C-terminus of p53 based on a similar approach (Zhu *et al.*, 2006), as shown in Figure 1A.

We found that fusion of a SUMO moiety to the C-terminus of p53 markedly attenuated its activity when compared with wild-type (wt) p53. In colony formation assays, in-frame fusion of SUMO-1 or -3 to p53 abolished p53-mediated suppression of clonogenic growth (Supplemental Figure S1). Luciferase reporter gene assays showed that the p53-SUMO fusion constructs were less active in activating various p53-responsive promoters (Supplemental Figure S2). Gene expression analysis demonstrated that the p53-SUMO fusions were essentially inactive in activating mRNA expression of endogenous p53 target genes under normal cell culture conditions or in the presence of doxorubicin, a genotoxic chemotherapeutic drug (Supplemental Figure S3). In contrast, an in-frame fusion of 12-kDa FK506-binding protein (FKBP; a cytosolic protein that binds to rapamycin) or FKBP12 and rapamycin-binding domain in the mTOR kinase (FRB; a domain of the mTOR kinase that forms a tight complex with the binary FKBP-rapamycin complex) to the p53 C-terminus did not attenuate its transactivation function (Supplemental Figure S4). In the rapamycin-inducible SUMOylation experiment, p53-2xFKBP

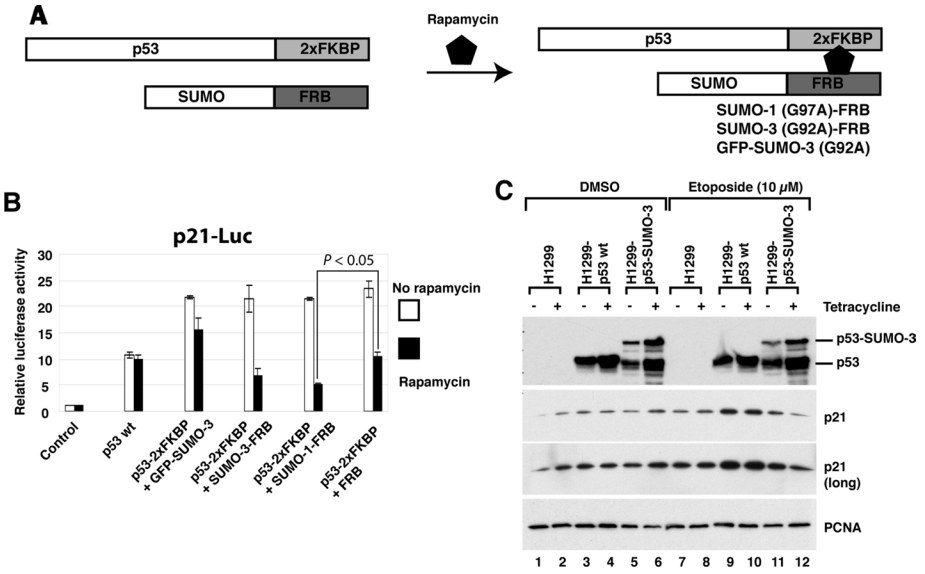

FIGURE 1: Rapamycin-mediated heterodimerization of p53 and SUMO inhibits p53 transactivation function. (A) Schematic diagram of p53-2xFKBP and fusion of SUMO-1 or -3 with FRB and their heterodimerization mediated by rapamycin. GFP-SUMO-3 served as a control. (B) Tethering SUMO to p53 inhibited its transactivation function. H1299 cells were transfected with a firefly luciferase reporter under the control of the *p21* promoter along with a control plasmid or various combinations of the indicated DNA constructs. The transfected cells were untreated (white bars) or treated with 0.1 μM of rapamycin at 6 h after transfection (black bars). Cells were lysed for dual luciferase assay 24 h after transfection. Statistical significance of pairwise comparisons was evaluated with Student's *t* test; down-regulation of reporter activity by heterodimerization of p53-2xFKBP and SUMO-1-FRB is significantly different from that by the control ($p < 0.05$). (C) p53-SUMO-3 fusion represses endogenous *p21* expression. H1299 cells were stably transduced with lentiviral vectors for tetracycline-inducible expression of wt p53 or p53-SUMO-3 fusion. The vehicle (dimethyl sulfoxide) or tetracycline was added to the parental H1299 cells and wt p53- and p53-SUMO-3–expressing cells as indicated. The cells were then exposed to vehicle or 10 μM etoposide for 18 h. The cells were lysed for Western blotting analysis with antibodies against the indicated proteins. PCNA was used as a loading control.

was highly active in activating the *p21* promoter in the absence of rapamycin. Although rapamycin did not affect wt p53 to activate the *p21* promoter, it markedly reduced the transactivation function of p53-2xFKBP when SUMO-1(G97A)-FRB or SUMO-3(G92A)-FRB was coexpressed (Figure 1B). Of note, although the direct fusion of FRB to the p53 C-terminus did not affect p53's ability to activate transcription (Supplemental Figure S4), rapamycin-mediated tethering of FRB to p53-2xFKBP also reduced p53-mediated activation of the *p21* promoter, although to a lesser extent than SUMO-1(G97A)-FRB or SUMO-3(G92A)-FRB (Figure 1B). To further assess potential impact of p53 SUMOylation on its function, we established cell lines with tetracycline-inducible expression of wt p53 and its fusion with SUMO-3. As shown in Figure 1C, under normal cell culture condition, the levels of p21 were similar in H1299 cells expressing wt p53 or p53-SUMO-3 in the absence or presence of tetracycline (lanes 3–6). In cells exposed to etoposide, however, a DNA-damaging chemotherapeutic agent, although p21 levels were markedly increased in cells expressing wt p53 (lanes 9 and 10), p21 expression was clearly repressed in cells expressing p53-SUMO-3 in a dose-dependent manner (lanes 11 and 12). Collectively SUMOylation of p53 inhibits its transactivation activity, consistent with previous findings (Wu and Chiang, 2009).

SUMO modification promotes nuclear export of p53

SUMOylation exerts diverse effects, ranging from regulation of transcription to intracellular trafficking (Gareau and Lima, 2010). Previous studies suggest that p53 SUMOylation enhances nuclear export of p53 (Carter *et al.*, 2007; Carter and Vousden, 2008; Heo *et al.*, 2011). To assess the potential effect of p53 SUMOylation on its intracellular localization in our experimental system, we immunostained p53 when it was fused to a SUMO moiety or when p53 was tethered to SUMO via rapamycin-induced heterodimerization in p53-null Saos-2 cells. As shown in Figures 2 and 3, wt p53 or its fusion with 2xFKBP was predominantly found in the nucleus, and rapamycin did not influence p53 nuclear localization (Figure 2A). By contrast, the p53-SUMO-1 fusion construct showed dramatic cytoplasmic presence (Figure 3A). In rapamycin-mediated heterodimerization experiments, coexpression of p53-2xFKBP with either SUMO-1-FRB or FRB did not influence p53 nuclear localization in the absence of rapamycin (Figure 2A). Remarkably, tethering SUMO-1-FRB but not the FRB control to p53-2xFKBP dramatically shifted p53 from the nucleus to the cytoplasm (Figure 2, A and B). Similar results were observed when SUMO-3 was fused to p53 or tethered to it via rapamycin-mediated heterodimerization (Figure 4). We further assessed whether rapamycin-mediated attachment of ubiquitin could also promote p53 nuclear export. We found that tethering ubiquitin to p53 did not obviously induce its nuclear export, although the heterodimerization of a ubiquitin moiety lacking lysine residues (K-less-Ub(G76A)-FRB–hemagglutinin [HA]) with p53-2xFKBP did trigger notable p53 nuclear export (Figure 5). Thus, in agreement with previous findings, monoubiquitination seems to enable nuclear export of p53 (Li *et al.*, 2003; Carter *et al.*, 2007). The signal intensity of nuclear p53, however, was still far greater than that of p53 in the cytoplasm in cells expressing p53-2xFKBP and K-less-Ub (G76A)-FRB-HA in the presence of rapamycin (Figure 5). Collectively these results support the notion that SUMOylation of p53 facilitates its nuclear export.

The SIM-binding pocket of SUMO is required for p53 nuclear export

Structural studies revealed that a specific hydrophobic groove on the surface of SUMO proteins mediates interactions with a SIM that is present in diverse SUMO-binding proteins (Song *et al.*, 2004; Reverter and Lima, 2005; Escobar-Cabrera *et al.*, 2010; Gareau and Lima, 2010; Chang *et al.*, 2011). This groove is composed of hydrophobic amino acid residues such as phenylalanine, tyrosine, valine, and leucine. The phenylalanine residue at position 36 (F36) and tyrosine 51 (Y51) in SUMO-1 and the corresponding residues in SUMO-3 are critical for interacting with a SIM (Song *et al.*, 2005; Sekiyama *et al.*, 2008).

To assess potential roles of the SIM-binding groove in the nuclear export of p53, we mutated F36 or Y51 of SUMO-1 to alanine. These mutated SUMO proteins were fused directly to the C-terminus of p53. As shown in Figure 3A, whereas the p53-SUMO-1 construct was present at high levels in the cytoplasm in ~90% of the transfected

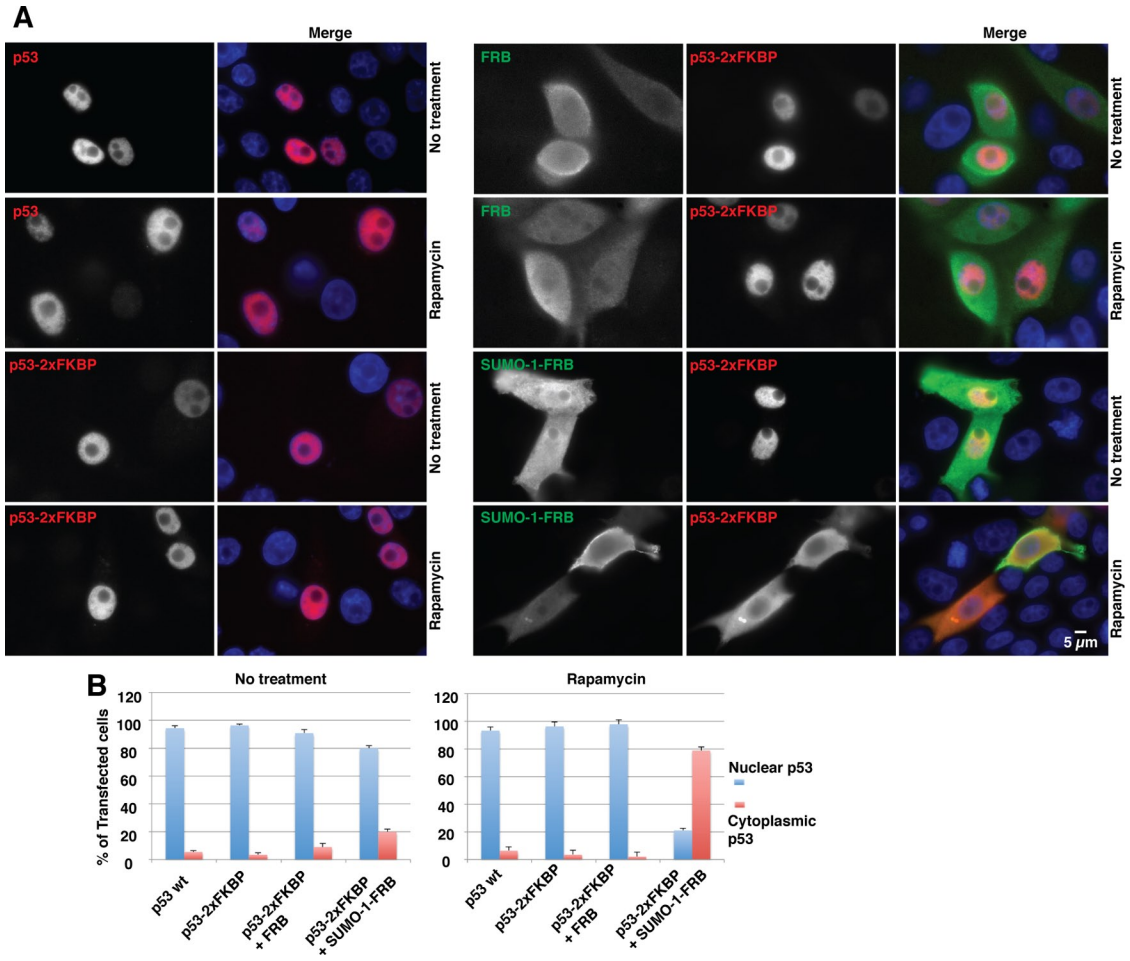

FIGURE 2: Rapamycin-mediated heterodimerization of p53 and SUMO promotes p53 nuclear export. (A) Saos-2 cells were transfected with the indicated DNA constructs. The transfected cells were untreated or treated with 0.1 μM rapamycin at 6 h after transfection. Cells were fixed for immunofluorescence microscopy 24 h after transfection. Representative images of transfected cells. (B) Quantification of p53 subcellular localization. Cells from at least 10 random microscopic fields that generally contained >200 transfected cells were examined for subcellular distribution of p53. Cells with predominant nuclear localization pattern of p53 with no visible cytoplasmic presence were counted as cells with nuclear p53, whereas those with predominant or clearly visible cytoplasmic distribution of p53 were counted as cells with cytoplasmic p53. Average percentage values of p53 subcellular distribution along with SDs.

cells, the mutation of either F36 or Y51 of SUMO-1 to alanine markedly impaired the cytoplasmic localization of the p53-SUMO-1 fusion. Fewer than 20% of the transfected cells expressing p53-SUMO-1(F36A) or p53-SUMO-1(Y51A) exhibited notable cytoplasmic presence of the fusion constructs (Figure 3A). To assess whether these p53-SUMO-1 constructs may express at different levels, we determined their expression in transfected Saos-2 cells using Western blotting. As shown in Figure 3A (right), the steady level of p53-SUMO-1(Y51A) was slightly lower than that of p53-SUMO-1, whereas that of the p53-SUMO-1(F36A) mutant was slightly higher. In cells expressing these three fusion constructs, the levels of endogenous SUMO-1, 2, and 3 were largely similar. Nonetheless, it appears that the levels of endogenous SUMO were moderately reduced in cells transiently expressing these three p53-SUMO-1 fusion constructs (lanes 2–4) compared with the control (lane 1). This is probably due to reduced transfection efficiency in the control, however, as the cotransfected GFP in the control was expressed at a lower level than that in cells cotransfected with any of these three p53-SUMO-1 fusions (Figure 3A). Thus the dramatically increased presence of p53-SUMO-1 in the cytoplasm in comparison to the two mutant fusion constructs was neither correlated with their expression levels nor due to their differential effects on endogenous SUMO levels.

Similarly, the rapamycin-mediated heterodimerization of SUMO-1(F36A)-FRB and p53-2xFKBP also failed to promote p53 nuclear export (Figure 3B). The results in Figure 3B show that p53 exhibited predominant nuclear localization in 70% of the transfected cells despite the presence of SUMO-1(F36A)-FRB and rapamycin. In contrast, nearly 60% of cells transfected with SUMO-1-FRB and p53-2xFKBP after the addition of rapamycin showed clear cytoplasmic localization of p53 (Figure 3B). These data are probably a conservative estimate, as we found that few if any cells expressing p53-2xFKBP and SUMO-1(F36A)-FRB in the presence of rapamycin exhibited predominant cytoplasmic location of p53. In most transfected cells with observable cytoplasmic p53, its nuclear staining intensity was still far greater than that in the cytoplasm (Figure 3B). Similarly, rapamycin-mediated heterodimerization of SUMO-3(F31A)-FRB with p53-2xFKBP also failed to induce p53 nuclear export (data not shown). Together, these results suggest that the hydrophobic SIM-binding groove of the SUMO moiety is critical for SUMO-mediated nuclear export of p53.

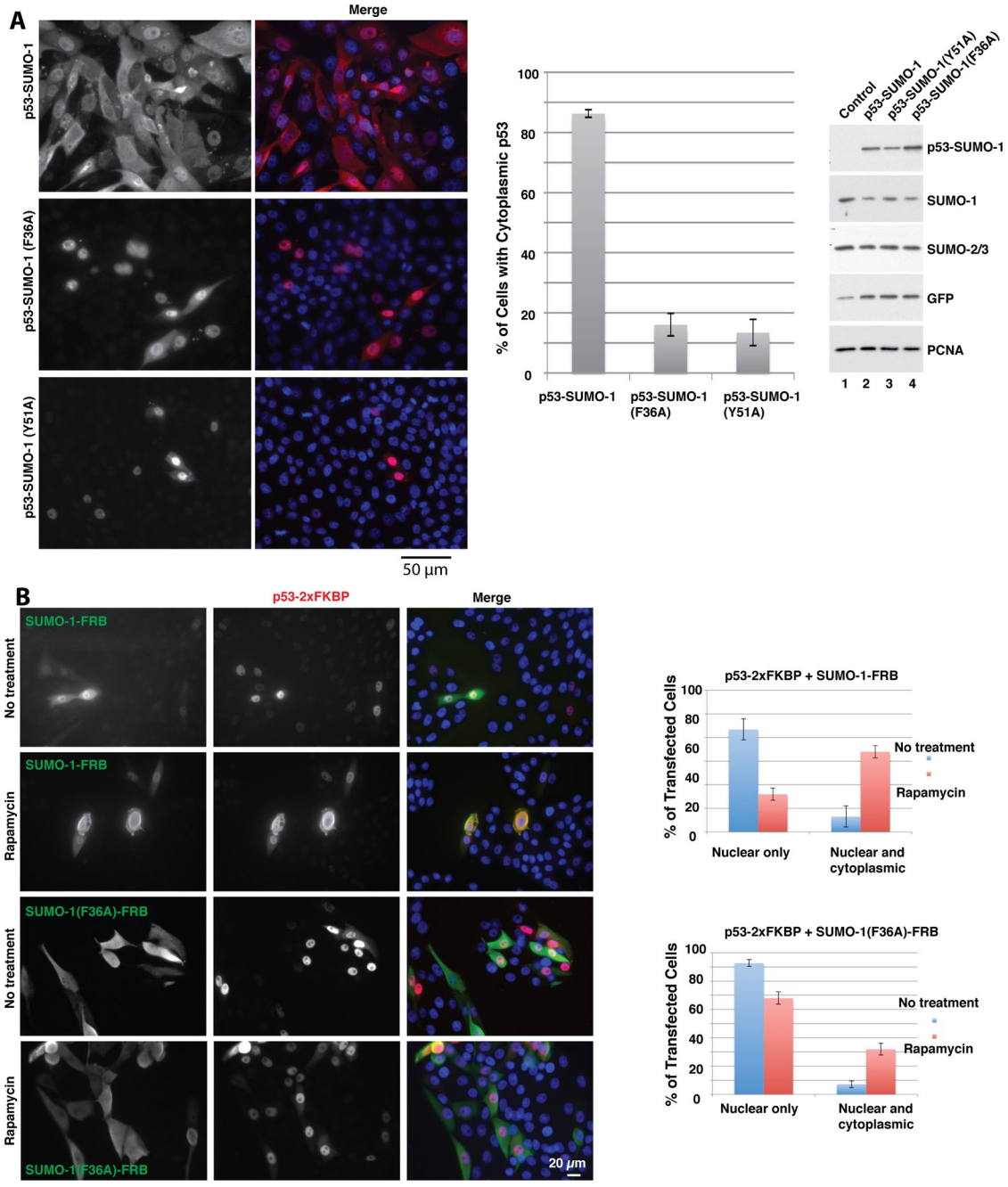

FIGURE 3: The SIM-binding groove of SUMO is required for nuclear exit of SUMO-modified p53. Saos-2 cells were transfected and processed for immunofluorescence microscopy as in Figure 2. Quantification of the subcellular distribution of p53 in transfected cells was determined as in Figure 2. (A) wt SUMO-1 or mutants with a mutation in the SIM-binding groove (F36A and Y51A) of SUMO-1 were directly fused to the C-terminus of p53. These fusion constructs were expressed in Saos-2 cells, and their intracellular distributions were examined. Representative images of cells expressing these constructs. Middle, plots depicting percentage distributions of these fusions. Western blotting was done to determine the expression levels of these p53-SUMO-1 fusion constructs in the transfected Saos-2 cells using an anti-p53 antibody (DO-1) and their effects on endogenous SUMO (right). GFP expression was used as a transfection control, and the PCNA level served as a loading control. (B) Representative images of cells expressing p53-2xFKBP along with SUMO-1-FRB or SUMO-1(F36A)-FRB in the absence or presence of rapamycin. Quantifications of p53 localizations (right).

SUMO attachment does not prevent p53 oligomerization

p53 has a canonical leucine-rich NES embedded in its tetramerization domain (Stommel *et al.*, 1999), which is inaccessible in the tetrameric or dimeric form of p53. The binding of this NES to CRM1 would require p53 oligomers to disassociate into the monomeric state. We described previously that tethering SUMO to p53 results in the nuclear export of p53. We thus wondered whether rapamycin-induced SUMO attachment to p53 would affect its tetramerization. To test this, we carried out immunoprecipitation (IP) experiments. We coexpressed FLAG-p53 with p53-2xFKBP (76-kDa) and

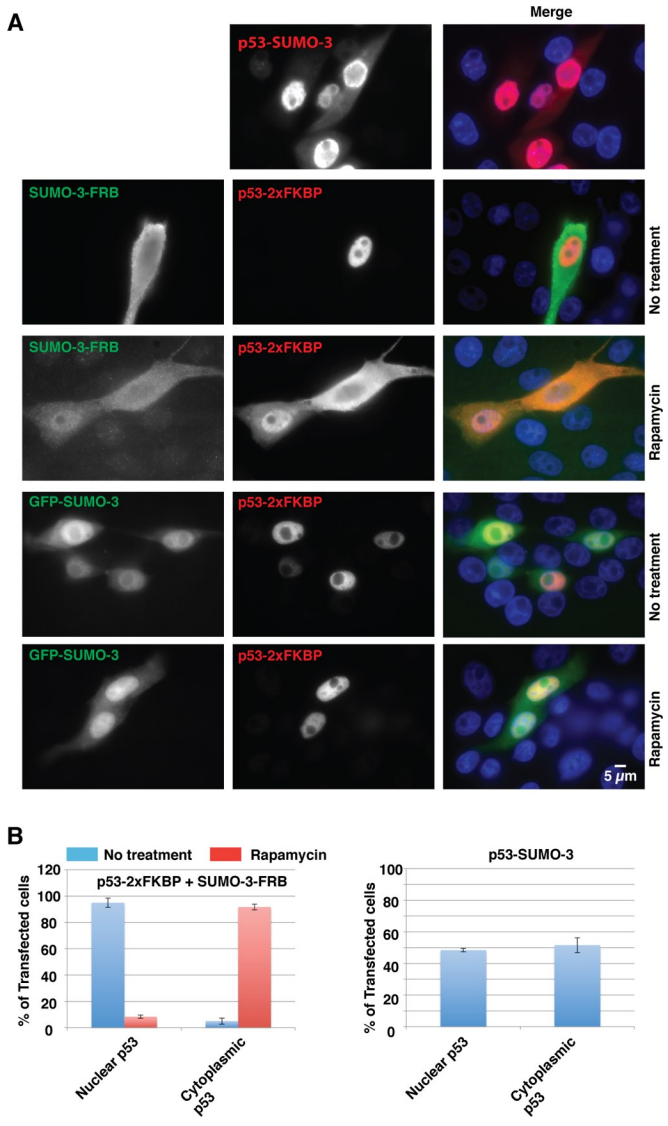

FIGURE 4: Tethering SUMO-3 to the C-terminus of p53 promoted its nuclear export. (A) Saos-2 cells were transfected with p53-SUMO-3 fusion or cotransfected with p53-2xFKBP or GFP-SUMO-3 along with FRB or SUMO-3-FRB constructs. One set of the transfected cells was exposed to rapamycin at 0.1 μM to induce heterodimerization 6 h after transfection. Immunofluorescence microscopy was done as in Figure 2. (B) Quantification of subcellular distributions of p53 in transfected cells as in Figure 2.

SUMO-3-FRB constructs. In the parallel control experiment, FLAG-p53 was coexpressed with GFP-p53 (78-kDa) and SUMO-3-FRB constructs. The transfected cells were either untreated or treated with rapamycin. The extracts of the transfected cells were subjected to IP using an anti-FLAG antibody conjugated to agarose beads. As shown in Figure 6A, both p53-2xFKBP (lane 1) and green fluorescent protein (GFP)–p53 (lane 4) were readily coprecipitated with FLAG-p53 in the absence of rapamycin. This suggested that FLAG-p53 could oligomerize with both p53-2xFKBP and GFP-p53, as expected. Similarly, in the presence of rapamycin, GFP-p53 was also coprecipitated with FLAG-p53 (Figure 6A, lane 8). Of note, in the presence of rapamycin, when p53-2xFKBP was chemically attached to SUMO-3-FRB, FLAG-p53 still coprecipitated with p53-2xFKBP (Figure 6A, lane 5). Of note, the levels of p53-2xFKBP appeared to be lower than that of GFP-p53 or FLAG-p53. This probably reflects inefficient detection of the p53-2xFKBP construct in Western blots, as comparable levels of both FLAG-p53 and p53-2xFKBP were observed in fluorescence micrographs (Figure 2A). These results suggested that rapamycin-mediated attachment of SUMO-3-FRB to p53-2xFKBP did not prevent the assembly of a p53 tetramer.

These experiments did not test whether SUMO-3-FRB-HA was indeed attached to the p53-2xFKBP construct in the presence of rapamycin. To evaluate this, we conducted similar IP experiments (Figure 6B). We transfected Saos-2 cells with FLAG-SUMO-3-FRB (with the FLAG tag at the N-terminus of SUMO-3-FRB), p53-2xFKBP, and HA-p53. As shown in Figure 6B, in the absence of rapamycin, a background amount of p53-2xFKBP and HA-p53 coprecipitated with FLAG-SUMO-3-FRB (lane 9). In contrast, much more p53-2xFKBP and HA-p53 coprecipitated in the presence of rapamycin (lane 11). In separate IP experiments, we also used SUMO-3-FRB-FLAG (with the FLAG epitope at the C-terminus of SUMO-3-FRB). Although the expression levels of p53-2xFKBP and HA-p53 appeared to be slightly lower when coexpressed with SUMO-3-FRB-FLAG (Figure 6B, lanes 6 and 8), it is clear that the presence of rapamycin resulted in more coprecipitation of both HA-p53 and p53-2xFKBP than in samples untreated with rapamycin (Figure 6B, compare lanes 12 and 10). Collectively these IP results confirm that p53 can still form oligomers when SUMO is attached to the C-terminus of p53.

CRM1 is required for SUMO-mediated nuclear export of p53

Although CRM1 is known to mediate the nuclear export of p53 (Stommel *et al.*, 1999), it is unknown whether the striking SUMO-provoked nuclear exodus of p53 also depends on CRM1. To address this, we cotransfected p53-SUMO-1 along with a control short hairpin RNA (shRNA) plasmid or one of two shRNAs targeting CRM1 and examined subcellular distributions of the p53-SUMO-1 construct in the transfected cells. In cells coexpressing the control shRNA and p53-SUMO-1, nearly 90% of the transfected cells showed clear or predominant cytoplasmic localization of p53. When a CRM1 shRNA was expressed in the transfected cells, however, the percentage of cells with cytoplasmic p53 was markedly reduced (Figure 7, A and B). We confirmed that the expression of both CRM1 shRNAs resulted in reduced CRM1 mRNA levels in the transfected cells (Figure 7C). Furthermore, data presented in Figure 8 show that SUMO-1 could no longer stimulate the nuclear export of the p53 mutants that could not interact with CRM1. The p53 mutant with the L348A/L350P double mutations in the tetramerization domain does not interact with CRM1, whereas the deletion of amino acid residues 11–27 (p53 del11-27) did not affect CRM1 to bind p53 (see discussion of Figure 9). Rapamycin-mediated heterodimerization of SUMO-1-FRB and p53 del11-27-2xFKBP induced p53 nuclear export (Figure 8, parts 11 and 12). In contrast, rapamycin-mediated tethering of SUMO-1-FRB to the p53-2xFKBP constructs containing the L348A/L350P double mutation failed to induce p53 nuclear export (Figure 8, parts 4–6 and 16–18). These data indicate that the CRM1-p53 interaction is indispensable for p53 nuclear export. Thus SUMO-mediated p53 nuclear export depends on CRM1.

CRM1 interacts with tetrameric form of p53

Structural studies show that a specific hydrophobic cleft in the toroid structure of CRM1 between HEAT repeats 11 and 12 interacts with the NES of a cargo, serving as a recognition signal for the CRM1–cargo interaction (Dong *et al.*, 2009; Monecke *et al.*, 2009). Although p53 carries a typical NES within the tetramerization domain

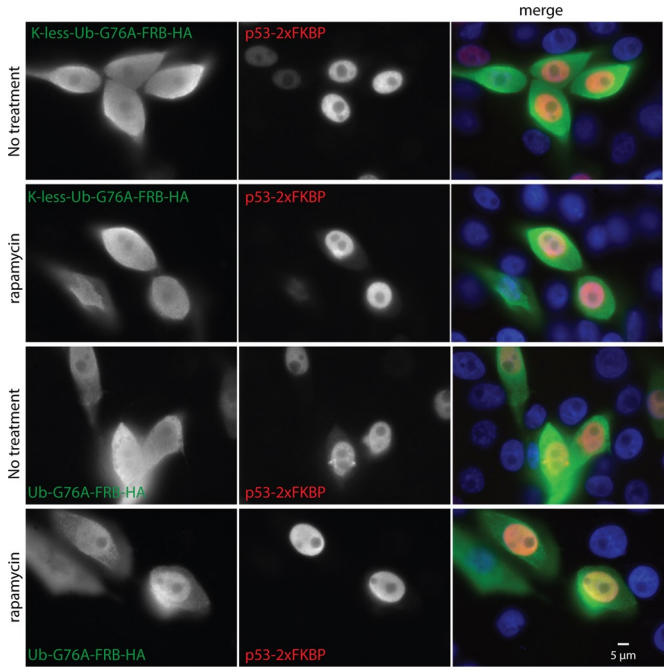

FIGURE 5: Effect of rapamycin-induced attachment of ubiquitin to p53 on its intracellular localization. Saos-2 cells were transfected with the indicated DNA constructs (p53-2xFKBP along with K-less-Ub(G76A)-FRB-HA or Ub(G76A)-FRB-HA). Cells were untreated or treated with rapamycin (0.1 μM) 6 h after transfection and fixed 24 h after transfection. Cells were stained with rabbit anti-HA and mouse anti-p53 (DO-1) antibodies. Goat anti-rabbit immunoglobulin G (IgG)–fluorescein and goat anti-mouse IgG-rhodamine conjugates were used as the secondary antibodies. The nuclei were stained with 4′,6-diamidino-2-phenylindole.

(Stommel *et al.*, 1999), the importance of this NES for p53-CRM1 interaction has not been examined experimentally. We used yeast two-hybrid assays to test the interactions between CRM1 constructs fused to the Gal4 transactivation domain (Gal4-AD) and p53 constructs fused to the Gal4 DNA-binding domain (Gal4-BD). As shown in Figure 9A, p53 interacted with CRM1 (amino acids [aa] 571–1071; Figure 9A, sector 2) but failed to bind a shorter C-terminal fragment (aa 910–1071) spanning from the HEAT repeat 19 to the C-terminus (sector 3), suggesting that the p53-binding sites reside within HEAT repeats 12–18 in CRM1. Of note, the hydrophobic groove in CRM1 that binds to a leucine-rich NES is not present in the CRM1 aa 571–1071 fragment (Dong *et al.*, 2009; Monecke *et al.*, 2009). These data thus suggest for the first time that the NES binding by CRM1 is not required for CRM1-p53 interaction.

To further assess the nature of the p53-CRM1 interaction, we tested various p53 constructs with mutations in different regions of the protein for binding to CRM1. Figure 9B shows that point mutations or deletion of the N-terminal transactivation domain, including the deletion of aa 11–27 that was shown to harbor a putative NES (Zhang and Xiong, 2001), did not affect p53-CRM1 interaction (Figure 9B and data not shown). Three key hydrophobic residues, L344, L348, and L350, within the NES in the p53 tetramerization domain are required for forming the p53 tetramer (Lee *et al.*, 1994; Jeffrey *et al.*, 1995; Waterman *et al.*, 1995; Mateu and Fersht, 1998). Indeed, any mutation of these residues has been shown to disrupt p53 oligomerization. The p53 L348A/L350P double mutant only forms monomer (Kawaguchi *et al.*, 2005), whereas p53 L344A forms dimers (Mateu and Fersht, 1998). Of interest, the monomeric p53 mutant failed to bind CRM1 (Figure 9B, row 3), whereas transformants containing the dimeric mutant (Gla4-AD-p53 L344A; Figure 9B, row 4) exhibited slightly impaired growth compared with wt p53 (Figure 9B, row 2), indicative of reduced affinity of dimeric p53 to CRM1. Truncation of the N-terminal 83 residues and the C-terminal tail (aa 356–393) of p53 did not obviously affect its interaction with CRM1 (Figure 9B, row 5). The p53 truncation mutant (aa 84–315) lacking the tetramerization domain, however, could no longer bind CRM1 (Figure 9B, row 6). We also tested the ability of several tumor-derived p53 mutants to interact with CRM1. Of interest, mutations within the DNA-binding domain (DBD, or core domain) of p53 exhibited differential effects on the p53-CRM1 interaction. Whereas R248W (Figure 9B, row 10) and R273H (row 11) mutants were able to bind CRM1, V143A (row 7) and R175H (row 9) mutants exhibited severely impaired binding to CRM1. Strikingly, in contrast to the R175H mutant, the mutation of R175 to Pro in p53 (R175P) did not notably affect p53-CRM1 interaction (Figure 9B, row 8). Structural studies demonstrated that p53 R248H and R273H mutants are so-called "contact" mutants, which do not alter the overall structure of the DBD but fail to bind DNA, whereas V143A and R175H represent "structural" mutations, which significantly change the tertiary folds of DBD (Cho *et al.*, 1994; Wong *et al.*, 1999). In contrast to the R175H mutant, the R175P mutant likely maintains the structural integrity of p53, as it remains active in transactivation (Liu *et al.*, 2004). These data indicate that the structural integrity of the core domain rather

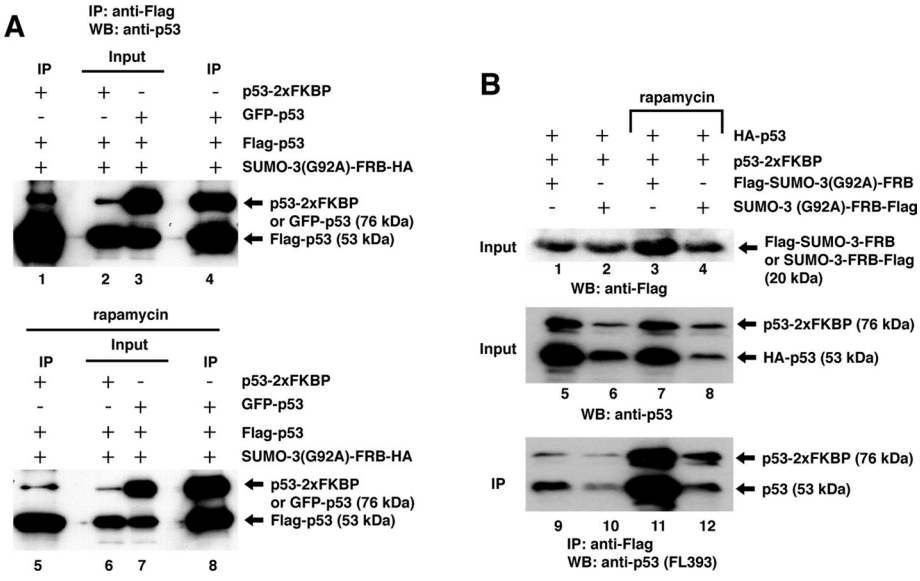

FIGURE 6: Coimmunoprecipitation of p53 and SUMO-modified p53. (A) Saos-2 cells were transfected with the indicated DNA constructs. The transfected cells were untreated or exposed to 0.1 μM rapamycin. At 24 h after transfection, cells were lysed and the extracts of the transfected cells were subjected to IP as described in *Materials and Methods*, and different forms of coprecipitated p53 were detected in Western blotting analysis. (B) Transfections with the specified DNA constructs, rapamycin treatment, and IP experiments were done as in A.

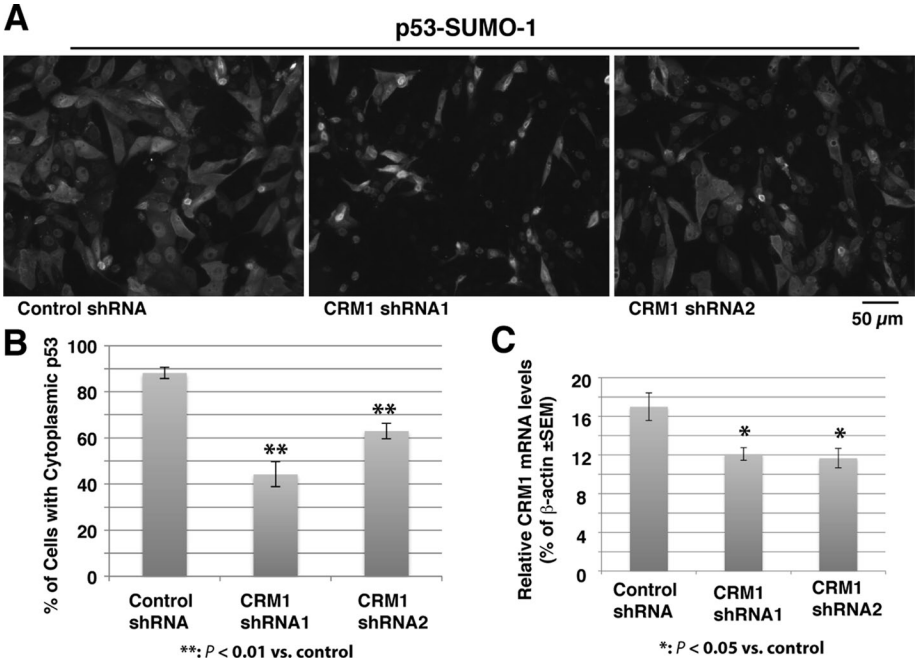

FIGURE 7: Effects of shRNA-mediated knockdown of CRM1 on SUMO-stimulated p53 nuclear export. (A) Saos-2 cells were cotransfected with the p53-SUMO-1 construct along with an indicated shRNA expression vector. Cells were fixed and subjected to immunofluorescence microscopy. Representative images of cells transfected with the indicated constructs. (B) Subcellular localization of p53 quantified as in Figure 2. Error bars are SEM. The *p* values of pairwise comparisons were calculated with Student's *t* tests. (C) Relative CRM1 mRNA levels in Saos-2 cells transfected with the indicated shRNA vectors were determined by quantitative real-time PCR. The results are average values of biological triplicate samples along with SEM. The *p* values were assessed with Student's *t* tests.

than the intrinsically unfolded N- or C-terminal tails of p53 is critically important for p53 to bind to CRM1.

Figure 8 shows that CRM1 failed to export p53 mutants that do not interact with it despite SUMO-1 attachment. These p53 mutants are defective in forming tetramer. Thus these results suggest that the importance of the p53 NES in the tetramerization domain for the p53-CRM1 interaction reflects the requirement of this sequence for maintaining the tetrameric form of p53 rather than its role in mediating a direct interaction with CRM1.

CRM1 contains SIM in the HEAT9 loop

Inspection of the primary sequence of CRM1 protein revealed several putative SIMs, as noted by others (Makhnevych *et al.*, 2009). One such element located within the long HEAT9 loop attracted our attention. This highly conserved motif in CRM1 contains a hydrophobic core consisting of the VLVV motif flanked by acidic residues (Figure 9C) that are characteristic of bona fide SIMs (Santiago *et al.*, 2009; Gareau and Lima, 2010). This motif assumes a β-strand configuration in various CRM1 crystal structures (Dong *et al.*, 2009; Monecke *et al.*, 2009, 2013; Koyama and Matsuura, 2010), similar to the structure of a typical SIM (Reverter and Lima, 2005). To test whether this motif indeed binds SUMO, we conducted yeast two-hybrid assays. Figure 9D shows that SUMO-1, but not the SUMO-1 F36A mutant, could bind full-length CRM1 (Figure 9D, sectors 2 and 3). We then tested a CRM1 fragment containing the putative SIM (aa 375–463) for interacting with SUMO-1. We found that SUMO-1 could bind to this CRM1 fragment (sector 5) but not to a similar construct with the V430K mutation within the hydrophobic core of this putative SIM (sector 6). Thus a functional SIM is present in the HEAT9 loop in CRM1.

Effect of p53 SUMOylation on p53-CRM1 interaction

Having shown that p53 SUMOylation promotes its nuclear export, we then assessed the potential influence of p53 SUMOylation on its interaction with CRM1. IP experiments showed little coprecipitation between wt p53 and CRM1 (Figure 10A, lane 9). Of interest, the mutation of the sole SUMO modification site K386 to Arg (K386R) increased binding of p53 to CRM1 (lane 10). Mutation of the SIM in the HEAT9 loop similarly enhanced p53-CRM1 interaction (lane 11). The interaction between p53 K386R and CRM1 V430K mutants was also readily detected (lane 12). These results suggest that p53 SUMOylation might destabilize the p53-CRM1 complex, and preventing p53 SUMOylation or inactivating the CRM1 HEAT9 SIM could stabilize this complex. We further tested the interaction between p53-SUMO-1 and CRM1. As shown in Figure 10B, p53-SUMO-1 formed a complex with CRM1, and a mutation of the HEAT9 SIM enhanced this interaction (Figure 10B, lanes 9 and 10). A mutation within the hydrophobic SIM-binding groove in the p53-SUMO-1 construct (p53-SUMO-1 F36A) similarly enhanced CRM1-p53 interaction (Figure 10B, lane 11). Strikingly, simultaneous mutations of the HEAT9 SIM of CRM1 (V430K) and the SIM-binding pocket in p53-SUMO-1 (p53-SUMO-1 F36A) markedly stabilized the p53-CRM1 complex (Figure 10B, lane 12). Thus it appears that the presence of a functional SIM in the HEAT9 loop of CRM1 and p53 SUMOylation serves to regulate the CRM1-p53 complex stability (see *Discussion*).

Previous studies demonstrated that mutations within the HEAT9 loop impair RanBD-mediated NES-substrate dissociation from CRM1 (Koyama and Matsuura, 2010) and the RanGTP-CRM1 interaction (Petosa *et al.*, 2004). We assessed effects of the CRM1 V430K mutant on p53 nuclear export. We found that wt CRM1 markedly increased and V430K mutant significantly decreased cytoplasmic localization of p53 (Figure 10C). This was not due to altered localization of the CRM1 V430K mutant, as both GFP-CRM1 and GFP-CRM1 V430K exhibited similar intracellular distributions, including localizations in the nuclear rim, cytoplasm, and nucleolus (Supplemental Figure S5).

Because the CRM1 V430K mutant and the p53-SUMO-1 (F36A) construct forms a stable complex, one consequence could be an accumulation of the CRM1-p53 complex at the NPCs. Furthermore, p53-SUMO-1 may remain stably associated with CRM1 in the cytoplasm even after the complex is released from the NPCs. To test this possibility, we coexpressed GFP-CRM1 or the V430K mutant with p53-SUMO-1 or a corresponding construct with a mutation in the SIM-binding pocket of SUMO-1 (F36A or Y51A). We observed striking colocalizations of p53 and CRM1 in a mesh of regularly spaced dots around the nuclear rim and across the entire span of the nucleus (Figure 11, A and B). This pattern is more apparent in cells expressing the CRM1 V430K mutant and one of the p53-SUMO-1 fusion with a mutated SIM-binding groove (Figure 11B; e.g., 1–3). The nuclear pore localization of the p53-SUMO-1/CRM1 complex was confirmed, as both p53-SUMO-1 and CRM1 V430K colocalized

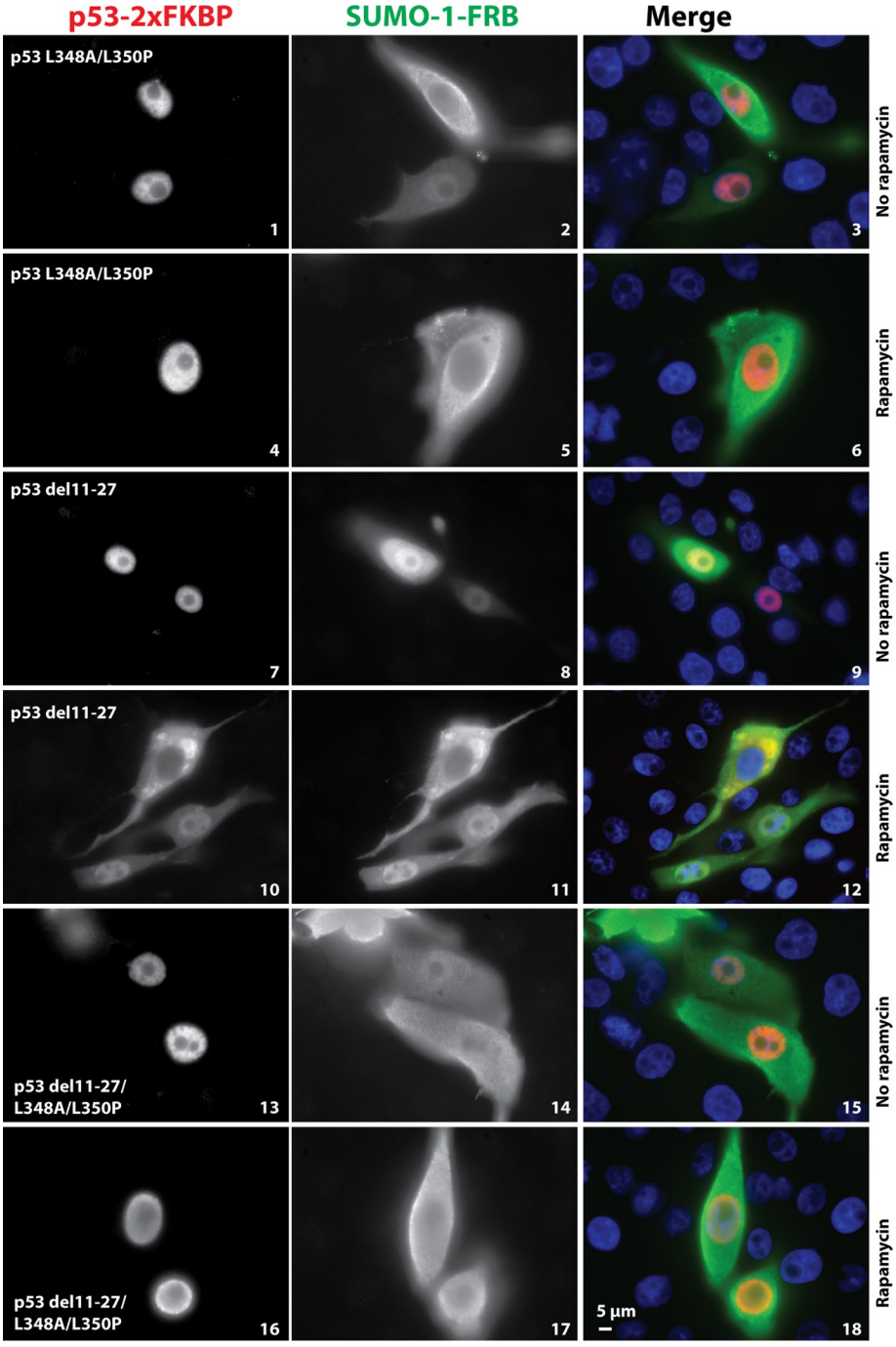

FIGURE 8: Tethering SUMO-1 to monomeric p53 failed to promote its nuclear export. Saos-2 cells were transfected with the indicated p53 constructs along with the SUMO-1-FRB-HA construct. p53 del11-27 contains a deletion of amino acid residues 11–27. The L348A/L350P double mutation within the tetramerization domain abolishes p53 oligomerization. The p53 del11-27/L348A/L350P construct carries both del11-27 deletion and the L348A/L350P double mutation. The transfected cells were untreated or exposed to rapamycin and then processed for immunostaining as in Figures 2 and 3.

with Nup153, a component of the NPC (Figure 11C, bottom, spots highlighted with white arrows). Colocalization of p53-SUMO-1, CRM1 V430K, and Nup153 was also obvious at a different focal plane in the same cell (Supplemental Figure S6). Remarkably, p53-SUMO-1/CRM1 V430K aggregates are clearly seen in the cytoplasm (Figure 11C, top; also see Figure 11, A and B, white arrows). The cytoplasmic p53-SUMO-1/CRM1 aggregates were observed in the vast majority (>80%) of the transfected cells that coexpressed GFP-CRM1 (V430K) mutant and any of the three p53-SUMO-1 fusions. Of interest, whereas several bright dots of p53-SUMO-1 appeared in the nucleus, CRM1 did not localize to those nuclear p53-SUMO-1 aggregates (Figure 11C, yellow arrow). Greater than 50% of the transfected cells contain nuclear aggregates of p53-SUMO-1, but none of these nuclear bodies colocalized with CRM1. Thus the stable p53-SUMO-1/CRM1 V430K mutant complex appears to reside only in the cytoplasm and not in the nucleoplasm.

DISCUSSION

The results reported here are consistent with a model in which SUMOylation of p53 or other cargo proteins weakens its affinity to the CRM1 exporter, resulting in efficient release of cargoes to the cytoplasm (Figure 11D). CRM1, RanGTP, and a cargo protein form a tight complex cooperatively in the nucleus. In this ternary complex, the HEAT9 loop wraps around RanGTP and partitions it to one corner of the interior in the CRM1 toroid (Monecke *et al.*, 2009; Koyama and Matsuura, 2010). The acidic residues in the HEAT9 loop interact with basic residues in the "switch I" of RanGTP and helices 12B–15B of CRM1 (Monecke *et al.*, 2009; Koyama and Matsuura, 2010). The HEAT9 loop also binds to a region of RanGTP in the loops involved in guanine recognition (Monecke *et al.*, 2009). Although the highly conserved hydrophobic residues in the HEAT9 loop are exposed to water in the RanGTP-CRM1-SPN1 ternary complex (Monecke *et al.*, 2009; Koyama and Matsuura, 2010), they are critical for the complex formation, as mutations of the hydrophobic residues to Asp or Glu residues completely abolish RanGTP-CRM1 interaction (Petosa *et al.*, 2004). The tight RanGTP-CRM1-cargo ternary complex is resistant to RanGAP1-activated GTP hydrolysis (Askjaer *et al.*, 1998; Petosa *et al.*, 2004). Therefore weakening this complex is important for cargo release and the conversion of RanGTP to RanGDP, thereby completing the irreversible step of cargo nuclear export.

We show here that the HEAT9 loop contains a bona fide SIM. We propose that cargo SUMOylation is mechanistically linked to cargo release. It can be envisioned that when the RanGTP-CRM1-cargo complex reaches the cytoplasmic side of the NPC, it interacts with the RanBP2 filaments (Hutten and Kehlenbach, 2007). The stable RanBP2/RanGAP-1*SUMO1/Ubc9 SUMO E3 ligase (Werner *et al.*, 2012) would efficiently SUMOylate a cargo such as p53. SUMOylated cargo then interacts with the SIM in the HEAT9 loop through the hydrophobic SIM-binding pocket in the SUMO moiety (Figure 11D). In various

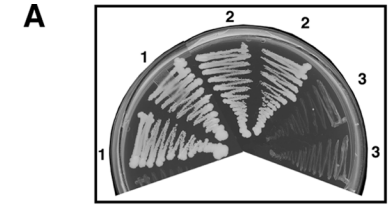

Sectors	Gal4-AD hybrid	Gal4-BD hybrid	Interaction
1	p53 Full-length	Mdm2 Full-length	Yes (positive control)
2	p53 Full-length	CRM1 aa 571-1071	Yes
3	p53 Full-length	CRM1 aa 910-1071	No

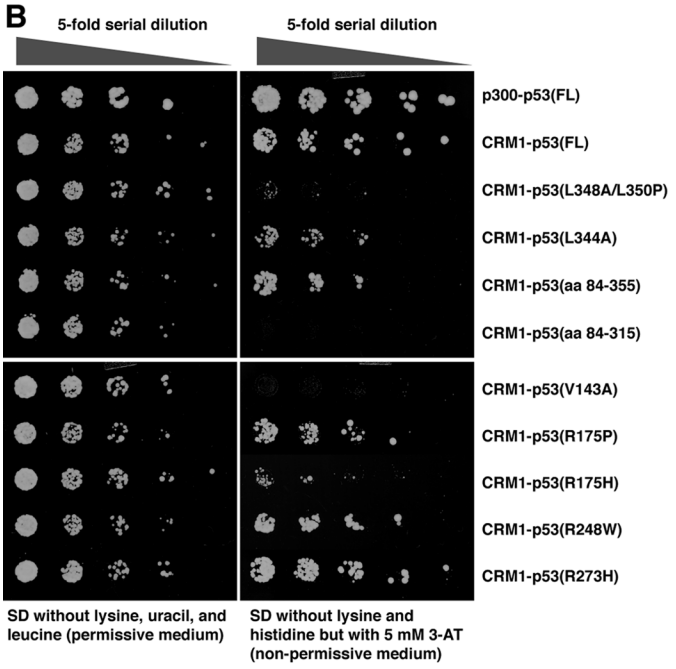

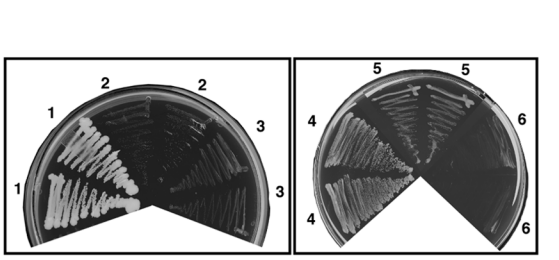

Sectors	Gal4-AD hybrid	Gal4-BD hybrid	Interaction
1	p53 full-length	MDM2 full-length	Yes (positive control)
2	SUMO-1	CRM1 full-length	Yes
3	SUMO-1 (F36A)	CRM1 full-length	No
4	p53-SUMO-1 fusion	Daxx full-length	Yes (positive control)
5	SUMO-1	CRM1 aa 375-463	Yes
6	SUMO-1	CRM1 aa 375-463 (V430K)	No

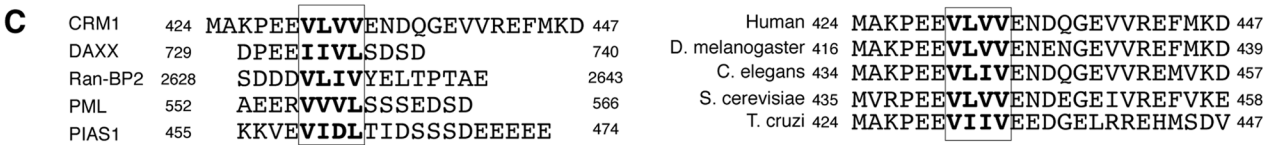

FIGURE 9: Interaction between p53 and CRM1 as determined in yeast two-hybrid assays. (A) The indicated CRM1 constructs fused to Gal4-BD were introduced to yeast cells along with various p53 constructs fused to Gal4-AD. The transformants of each hybrid combination were restreaked in duplicate on plates with SD medium lacking lysine and histidine. Yeast two-hybrid assays of the Gal4-BD-Mdm2 construct with Gal4-AD-p53 hybrid were done as a positive control (sector 1). (B) Yeast cells were transformed with the indicated combinations of Gal4-AD-p53 and Gal4-BD-CRM1 (aa 571–1071) hybrids. The resulting transformants were grown overnight in the permissive medium (SD lacking lysine, leucine, and uracil) at 30°C. The overnight cultures were serially diluted and plated on the permissive medium (left) and nonpermissive medium (SD lacking histidine and lysine; right). The transformation with Gal4-BD-p300 and Gal4-AD-p53 was used as a positive control (first row). Representative results of at least two distinct colonies with similar growth phenotype for each combination. (C) Sequence alignments of the HEAT9 loop of CRM1 with known SIMs from the indicated human proteins (left) and among the corresponding HEAT9 loop sequences of various CRM1 orthologues from the indicated species (right). The hydrophobic core of the SIMs is boxed. The numbers in each sequence refer to beginning and ending residues in each protein. (D) Full-length CRM1 or a fragment encompassing aa 375–463 (HEAT9 loop) fused to Gal4-BD was tested for interaction with indicated SUMO constructs fused to Gal4-AD. Yeast two-hybrid assays were done as in A.

structures of SIM-SUMO complexes, the hydrophobic core of a SIM interacts with the hydrophobic interior of the SIM groove on the surface of SUMO. The acidic residues flanking the hydrophobic core interact with basic residues surrounding the SIM groove (Reverter and Lima, 2005; Chang *et al.*, 2011; Ullmann *et al.*, 2012). Thus recognition of the SIM of the HEAT9 loop probably breaks the critical contacts between CRM1 and RanGTP, which is likely to facilitate the dissociation of RanGTP from CRM1 (Figure 11D). SUMOylated cargoes might quickly undergo deSUMOylation by NPC-associated SUMO-specific proteases such as SENP2 (Goeres *et al.*, 2011).

Our data indicate that p53 binds to CRM1 between HEAT repeats 12 and 18 (Figure 9). Of interest, the tetrameric form of p53 is required for this interaction. The intrinsically disordered N- and C-terminal tails of p53 are dispensable for CRM1 to bind p53. Surprisingly, proper folding of the p53 core domain seems essential for p53-CRM1 interaction (Figure 9). In the crystal structures of the ternary RanGTP-CRM1-SPN1 complex, whereas the NES of SPN1 binds to a hydrophobic groove formed by helices 11A and 12A of CRM1, there are extensive interactions in a very large interface consisting of basic patches from SPN1 and multiple acidic residues from CRM1 between HEAT repeats 13A, 14A, and 14B (Dong *et al.*,

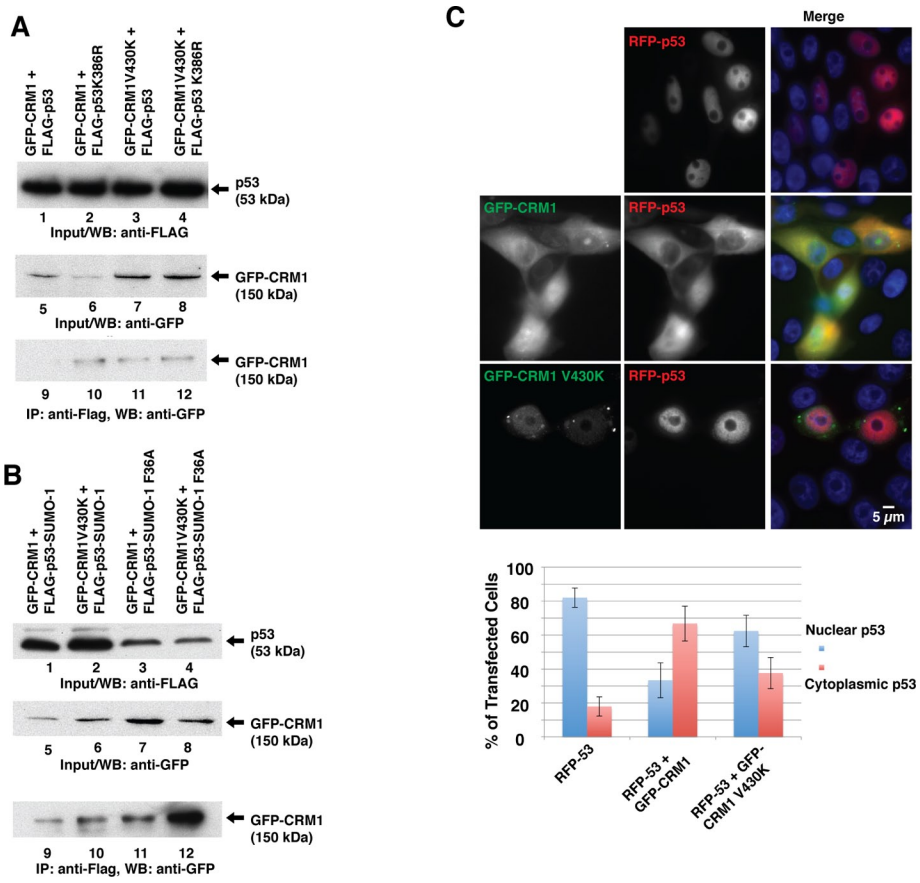

FIGURE 10: Effects of p53 SUMO modification on its interaction with CRM1. (A) Saos-2 cells were transfected with the indicated DNA constructs. The extracts of the transfected cells were subjected to IP as in Figure 6. Coprecipitated GFP-CRM1 was detected with an anti-GFP antibody. (B) The indicated DNA constructs were transfected into Saos-2 cells. IP assays and Western blotting were done as in A. (C) Saos-2 cells were transfected with RFP-p53 alone or together with GFP-CRM1 or GFP-CRM1 V430K as indicated. Cells were fixed for fluorescence microscopy 24 h after transfection as in Figure 2. Representative images are shown. Quantifications of subcellular distribution of p53 were done as in Figure 2 (bottom).

2009). Additional acidic patches on the vast convex surface formed by the HEAT repeats 13–20 in CRM1 are available for a cargo protein to dock. We speculate that proper orientation of the basic patches on the surface of the p53 core domain is critical for it to dock to the acidic surface of CRM1. Thus tumor-derived mutations that impair correct folding of the core domain would prevent p53 from binding to CRM1. Of note, many basic residues of SPN1 involved in interacting with CRM1 are from the structural elements surrounding the nucleotide-binding site in SPN1 (Dong *et al.*, 2009). It is possible that basic residues of p53 found in direct contact with DNA in the crystal structure of a p53-DNA complex (Cho *et al.*, 1994) might also be important for binding to CRM1. Further experiments will be required to test this idea.

The canonical leucine-rich NES in p53 is embedded in the tetramerization domain of p53 (Stommel *et al.*, 1999). Binding of this NES to the hydrophobic groove between helices 11B and 12B would require tetrameric p53 to dissociate into monomers. Previous studies indicated that monoubiquitination of the p53 C-terminal domain seems to increase the concentration of monomeric p53 (Carter *et al.*, 2007). Of interest, Mdm2 seems to promote p53 nuclear export independently of SUMOylation, as Mdm2 could still enhance the nuclear export of the p53 K386R mutant, which lacks the SUMO modification site. By contrast, enhancement of p53 nuclear export by PIASy, a known SUMO E3 ligase, seems to depend on the presence of K386 of p53 (Carter *et al.*, 2007). Thus it appears that there might be two independent p53 nuclear export pathways: one mechanism involves Mdm2-mediated monoubiquitination and enables the exposure of the C-terminal NES of p53, and the other is promoted by p53 SUMOylation and could export the tetrameric form of p53. We speculate that the SUMOylation-dependent export pathway might rely on the RanBP2/RanGAP-1*SUMO-1/Ubc9 E3 SUMO ligase complex for disassembly of the RanGTP-CRM1-cargo ternary complex, whereas cargo release in the SUMO-independent pathway might be mediated through RanBP1 (Hutten and Kehlenbach, 2007; Koyama and Matsuura, 2010). Our data suggest that SUMOylation-mediated p53 nuclear export appears to be more efficient than that mediated through monoubiquitination (Figures 2–5).

Proper regulation of p53 nuclear export has important functional consequences. In response to diverse cellular stress signals such as DNA damage, p53 accumulates in the nucleus and executes transcriptional programs to halt cell proliferation or promote cell death. Stress signals promote posttranslational modifications of p53, including the phosphorylation of multiple Ser and Thr residues and acetylation of several lysine residues (Dai and Gu, 2010). Such posttranslational modifications may play a major role in blocking p53 nuclear export (Zhang and Xiong, 2001). As discussed earlier, proper folding of the p53 core domain and the availability of a positively charged surface might be critical for p53 to bind CRM1. Both phosphorylation and acetylation result in a net loss of positive charges, thereby likely weakening p53-CRM1 interaction. Of note, many tumor-derived p53 mutations result in accumulation of p53 in the nucleus. Because the correctly folded core domain of p53 is important for it to bind to CRM1 (Figure 9), accumulation of such structural p53 mutants might partly be due to their diminished CRM1-mediated nuclear export. Of interest, the mutation of K351 to Asn (K351N) in the tetramerization domain of p53 results in its nuclear accumulation (Muscolini *et al.*, 2009). This mutation seems to contribute to cisplatin resistance in an ovarian cancer cell line due to decreased nuclear export and p53-mediated apoptosis in the cytoplasm (Muscolini *et al.*, 2011). Because the K351N mutant could still form dimers but not tetramers (Muscolini *et al.*, 2009), we predict that this p53 mutant will have impaired interaction with CRM1, accounting for its diminished nuclear export.

In summary, our studies provide some new insights into the regulatory roles of SUMOylation during nuclear export and the nature of the CRM1-p53 interaction. CRM1 binds to the tetrameric form of p53 with the properly folded p53 core domain. We demonstrated that p53 SUMOylation dramatically increased its nuclear export. SUMOylation of cargoes such as p53 appears to facilitate the disassembly of the ternary export complex by disengaging the HEAT9 loop of CRM1 from RanGTP.

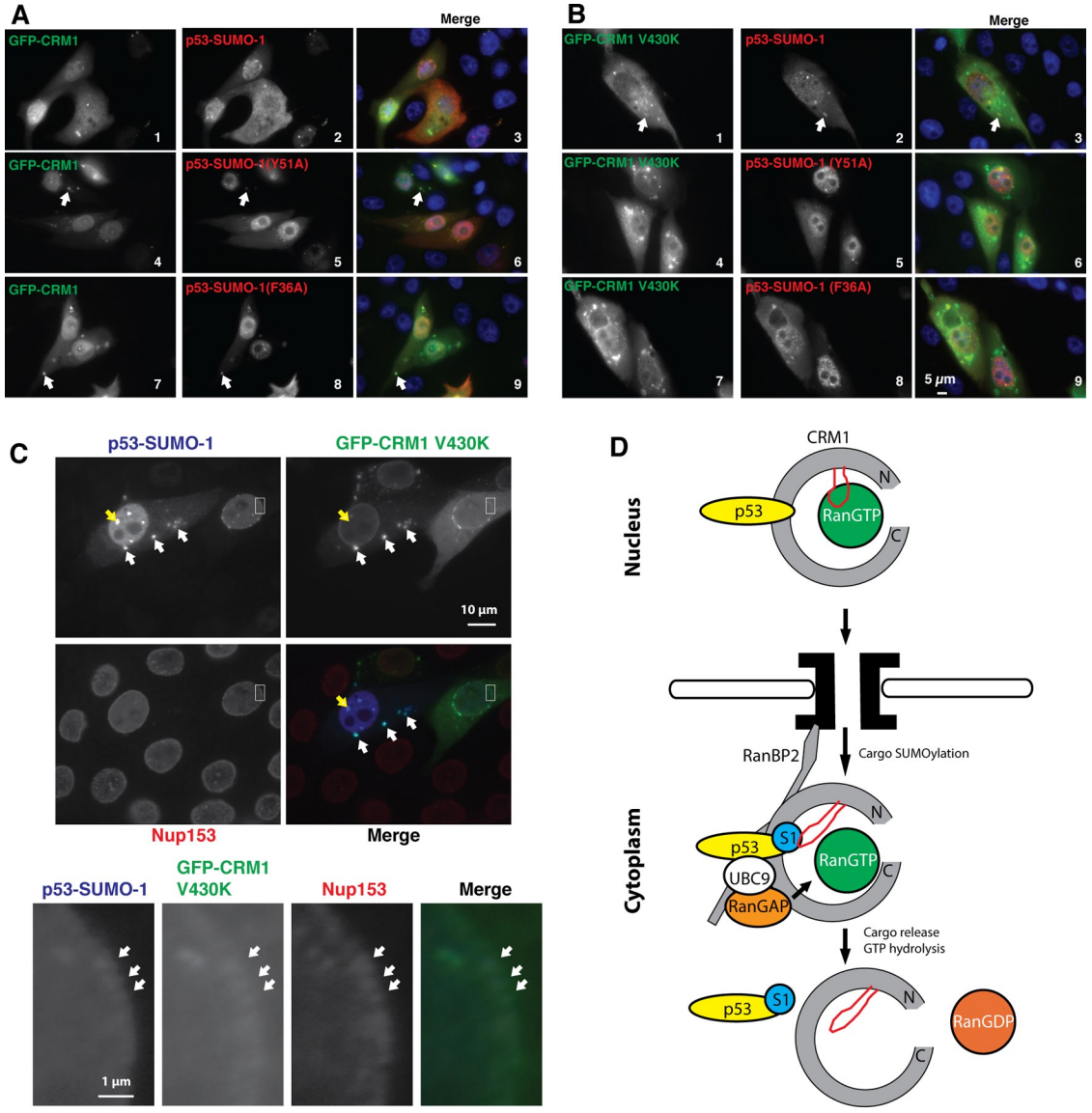

FIGURE 11: Effect of mutations in the SIM-binding groove of the p53-SUMO-1 fusion and the HEAT9 loop of CRM1 on their localization at NPCs. (A) The GFP-CRM1 (full-length) construct was cotransfected with an indicated p53-SUMO-1 fusion construct to Saos-2 cells. The transfected cells were fixed for immunofluorescence microscopy as in Figure 2. (B) The GFP-CRM1 (full-length) V430K mutant was cotransfected with an indicated p53-SUMO-1 fusion construct into Saos-2 cells. The transfected cells were fixed for immunofluorescence microscopy as described. (C) The p53-SUMO-1 fusion construct was coexpressed with the GFP-CRM1 V430K mutant in Saos-2 cells. The transfected cells were fixed 24 h after transfection and stained with antibodies to p53 and Nup153. p53, CRM1, and Nup153 were detected in the blue, green and red channels, respectively. Colocalization of CRM1, p53-SUMO-1, and Nup153 at the NPCs, as well as that of CRM1 and p53-SUMO-1 in the cytoplasm, is denoted with white arrows. Bottom, images of NPC colocalization of p53-SUMO-1, CRM1 V430K mutant, and Nup153 shown at a higher magnification, corresponding to the boxed area at the top. Lack of colocalization of CRM1 with the bright spots of p53-SUMO-1 in the nucleoplasm is indicated with a yellow arrow. (D) A model explaining a potential regulatory role for the cargo SUMOylation in cargo release and the disassembly of a CRM1 export complex. p53 (tetramer) is shown as the cargo (yellow oval). The HEAT9 loop is depicted as a hairpin in red. N, N-terminus; C, C-terminus; S1, SUMO-1. See the text for details.

MATERIALS AND METHODS

Materials, reagents, and cell lines

Vectors (PC4-RHE, pC4EN-F1, and pC4EN-F2) for making p53-2xFKBP and SUMO-FRB fusion constructs were from Ariad Technologies (Cambridge, MA). SUMO-1(G97A)-FRB-HA (SUMO-1-FRB) was from Michael Matunis (Johns Hopkins University, Baltimore, MD). Rapamycin and anti-FLAG M2-agarose were from Sigma-Aldrich (St. Louis, MO). Antibodies against p53 (DO-1 and FL-393) and the HA tag (Y-11) were from Santa Cruz Biotechnology (Santa Cruz, CA). Anti-FLAG rabbit polyclonal and mouse monoclonal antibodies were from Sigma-Aldrich. Anti-GFP mouse monoclonal antibody was from Babco (Berkeley, CA). The endogenous SUMO-1, and SUMO-2/SUMO-3 were detected with anti-SUMO-1 (FL-101; Santa Cruz Biotechnology) and 8A2 (Zhang *et al.*, 2008) from the Developmental Studies Hybridoma Bank (University of Iowa, Iowa City, IA). The anti–proliferating cell nuclear antigen (PCNA; 2714-1)

antibody was from Epitomics (Burlingame, CA). Human cancer cell lines (Saos-2 and H1299) were from the American Type Culture Collection (Manassas, VA) and cultured in DMEM supplemented with 10% bovine calf serum and 1% penicillin/streptomycin antibiotics and incubated at 37°C in an atmosphere with 5% CO_2. The shRNA clones targeting CRM1 (TRCN0000152787 and TRCN0000153235) were from Open Biosystems (Huntsville, AL). The control shRNA clone targeting firefly luciferase was cloned into a lentiviral vector (Zhao *et al.*, 2007) under the control of the human U6 promoter.

Immunofluorescence microscopy

Cells grown on glass coverslips were transfected with relevant DNA constructs. Rapamycin at 0.1 μM in dimethyl sulfoxide was added 6 h after transfection to induce heterodimerization. At 24 h after transfection, the cells were washed with phosphate-buffered saline (PBS) and fixed with 3% paraformaldehyde (in PBS with 0.1 mM $MgCl_2$ and 0.1 mM $CaCl_2$). They were permeabilized with 0.2% Triton X-100 (in PBS), washed twice with PBS, and blocked with a blocking solution (PBS containing 2% fetal bovine serum, 0.1% sodium azide, 0.1% Tween 20). The cells were then incubated sequentially with primary and secondary antibodies conjugated to a relevant fluorescent dye. The coverslips were mounted on glass slides using a mounting medium with 4′,6-diamidino-2-phenylindole. The cells were examined with a Zeiss Axiophot microscope (Carl Zeiss, Jena, Germany), and images were acquired with a charge-coupled device camera.

Yeast two-hybrid assays

Relevant DNA fragments of CRM1 open reading frames (ORFs) were fused to the Gal4 DNA-binding domain (BD) in plasmids pGBDU-C(x), and p53 ORF fragments were fused to the Gal4 activation domain (AD) in plasmids pGAD-C(x). Site-specific mutations of CRM1, SUMO, and p53 were made using QuikChange protocol (Stratagene, Santa Clara, CA). Yeast two-hybrid assays were conducted as described (Liu *et al.*, 2000). To assess the growth phenotype of yeast cells transformed with a combination of two-hybrid constructs, overnight cultures grown on the liquid yeast selective dropout (SD) medium without lysine, leucine, and uracil were initially diluted based on optical density readings at 600 nm and then diluted in fivefold serial dilutions. The diluted cells were stamped on an appropriate SD medium agar plate.

Immunoprecipitation

Cells were lysed in situ with cold buffer B (20 mM Tris-HCl, pH 8.0, 5 mM $MgCl_2$, 10% glycerol, 0.1% NP-40, 150 mM KCl, and 100-fold diluted protease inhibitor cocktails [P8340; Sigma-Aldrich]). Lysate was frozen at −80°C and then thawed at room temperature. Lysate was rotated at 4°C for 30 min and cleared by centrifugation. The cleared lysate was incubated with Anti-FLAG M2-agarose beads pretreated with 0.1 M glycine (pH 2.5). The mixture was rotated at 4°C for 2 h. The beads were recovered by centrifugation and washed four times with cold buffer B. Bound proteins were eluted by incubating with buffer B containing 0.1 mg/ml FLAG peptide at 4°C for 1 h with rotation or boiling directly in 2× SDS sample buffer. Samples were analyzed by Western blotting.

Luciferase reporter gene assays

The firefly luciferase reporter driven by a p53 target gene promoter (*p21*, *PUMA*, *Mdm2*, *PIG3*, *Fas*, *AIP*, or *PIDD*) was used. The reporters, along with a sea pansy (*Renilla reniformis*) luciferase reporter, were transiently transfected into H1299 cells. Each transfection was done in duplicate. Dual luciferase reporter assays were conducted 24 h after transfection. The firefly luciferase activities were normalized against that of the sea pansy.

Quantitative real-time PCR

Saos-2 cells cultured in a six-well plate were transfected with a control or a CRM1-specific shRNA vector in triplicate. At 24 h after transfection, total RNAs were extracted from the transfected cells using the RNeasy minikit (Qiagen, Valencia, CA). The RNA samples were then subjected to reverse transcription. The resulting cDNAs were used as templates for quantitative real-time PCR with the SYBR green detection method. In each sample, the CRM1 RNA levels were normalized to those of β-actin. The normalized RNA levels in cells expressing a CRM1 shRNA were compared with those in cells transfected with the control shRNA. The following PCR primer pairs (5′ to 3′) were used: CATTGTTTCCCAGCATTCCT (CRM1 forward), CGTATCTGCGACATTCCTCA (CRM1 reverse), GCTCCTCCTGAGCGCAAGTACTC (β-actin forward), and GTGGACAGCGAGGCCAGGAT (β-actin reverse).

ACKNOWLEDGMENTS

We thank Michael Matunis, Xiang-Jiao Yang, Thierry Soussi, and Ariad Technologies for providing various DNA clones, Kyle Roux for providing a monoclonal antibody against Nup153, and Jennifer Liao for helpful editing of the manuscript. Dawei Li was supported by a scholarship from the China Scholarship Council. This work was supported by grants from the National Cancer Institute (R01-CA092236) and the Bankhead-Coley Cancer Research Program of the Florida Department of Health (09BW-05-26823 and 09BB-11).

REFERENCES

Askjaer P, Jensen TH, Nilsson J, Englmeier L, Kjems J (1998). The specificity of the CRM1-Rev nuclear export signal interaction is mediated by RanGTP. J Biol Chem 273, 33414–33422.

Bischoff FR, Klebe C, Kretschmer J, Wittinghofer A, Ponstingl H (1994). RanGAP1 induces GTPase activity of nuclear Ras-related Ran. Proc Natl Acad Sci USA 91, 2587–2591.

Carter S, Bischof O, Dejean A, Vousden KH (2007). C-terminal modifications regulate MDM2 dissociation and nuclear export of p53. Nat Cell Biol 9, 428–435.

Carter S, Vousden KH (2008). p53-Ubl fusions as models of ubiquitination, sumoylation and neddylation of p53. Cell Cycle 7, 2519–2528.

Chang CC *et al.* (2011). Structural and functional roles of Daxx SIM phosphorylation in SUMO paralog-selective binding and apoptosis modulation. Mol Cell 42, 62–74.

Chen L, Chen J (2003). MDM2-ARF complex regulates p53 sumoylation. Oncogene 22, 5348–5357.

Cho Y, Gorina S, Jeffrey PD, Pavletich NP (1994). Crystal structure of a p53 tumor suppressor-DNA complex: understanding tumorigenic mutations. Science 265, 346–355.

Cook AG, Conti E (2010). Nuclear export complexes in the frame. Curr Opin Struct Biol 20, 247–252.

Dai C, Gu W (2010). p53 post-translational modification: deregulated in tumorigenesis. Trends Mol Med 16, 528–536.

Dawlaty MM, Malureanu L, Jeganathan KB, Kao E, Sustmann C, Tahk S, Shuai K, Grosschedl R, van Deursen JM (2008). Resolution of sister centromeres requires RanBP2-mediated SUMOylation of topoisomerase IIalpha. Cell 133, 103–115.

Dong X, Biswas A, Suel KE, Jackson LK, Martinez R, Gu H, Chook YM (2009). Structural basis for leucine-rich nuclear export signal recognition by CRM1. Nature 458, 1136–1141.

Escobar-Cabrera E, Lau DK, Giovinazzi S, Ishov AM, McIntosh LP (2010). Structural characterization of the DAXX N-terminal helical bundle domain and its complex with Rassf1C. Structure 18, 1642–1653.

Fischer U, Huber J, Boelens WC, Mattaj IW, Luhrmann R (1995). The HIV-1 Rev activation domain is a nuclear export signal that accesses an export pathway used by specific cellular RNAs. Cell 82, 475–483.

Fornerod M, Ohno M, Yoshida M, Mattaj IW (1997). CRM1 is an export receptor for leucine-rich nuclear export signals. Cell 90, 1051–1060.

Gareau JR, Lima CD (2010). The SUMO pathway: emerging mechanisms that shape specificity, conjugation and recognition. Nat Rev Mol Cell Biol 11, 861–871.
Goeres J, Chan PK, Mukhopadhyay D, Zhang H, Raught B, Matunis MJ (2011). The SUMO-specific isopeptidase SENP2 associates dynamically with nuclear pore complexes through interactions with karyopherins and the Nup107-160 nucleoporin subcomplex. Mol Biol Cell 22, 4868–4882.
Gostissa M, Hengstermann A, Fogal V, Sandy P, Schwarz SE, Scheffner M, Del Sal G (1999). Activation of p53 by conjugation to the ubiquitin-like protein SUMO-1. EMBO J 18, 6462–6471.
Guttler T, Gorlich D (2011). Ran-dependent nuclear export mediators: a structural perspective. EMBO J 30, 3457–3474.
Heo KS *et al*. (2011). PKCzeta mediates disturbed flow-induced endothelial apoptosis via p53 SUMOylation. J Cell Biol 193, 867–884.
Hutten S, Kehlenbach RH (2007). CRM1-mediated nuclear export: to the pore and beyond. Trends Cell Biol 17, 193–201.
Jeffrey PD, Gorina S, Pavletich NP (1995). Crystal structure of the tetramerization domain of the p53 tumor suppressor at 1.7 angstroms. Science 267, 1498–1502.
Kahyo T, Nishida T, Yasuda H (2001). Involvement of PIAS1 in the sumoylation of tumor suppressor p53. Mol Cell 8, 713–718.
Kawaguchi T, Kato S, Otsuka K, Watanabe G, Kumabe T, Tominaga T, Yoshimoto T, Ishioka C (2005). The relationship among p53 oligomer formation, structure and transcriptional activity using a comprehensive missense mutation library. Oncogene 24, 6976–6981.
Klein UR, Haindl M, Nigg EA, Muller S (2009). RanBP2 and SENP3 function in a mitotic SUMO2/3 conjugation-deconjugation cycle on Borealin. Mol Biol Cell 20, 410–418.
Koyama M, Matsuura Y (2010). An allosteric mechanism to displace nuclear export cargo from CRM1 and RanGTP by RanBP1. EMBO J 29, 2002–2013.
Lee W, Harvey TS, Yin Y, Yau P, Litchfield D, Arrowsmith CH (1994). Solution structure of the tetrameric minimum transforming domain of p53. Nat Struct Biol 1, 877–890.
Li M, Brooks CL, Wu-Baer F, Chen D, Baer R, Gu W (2003). Mono- versus polyubiquitination: differential control of p53 fate by Mdm2. Science 302, 1972–1975.
Liu G, Parant JM, Lang G, Chau P, Chavez-Reyes A, El-Naggar AK, Multani A, Chang S, Lozano G (2004). Chromosome stability, in the absence of apoptosis, is critical for suppression of tumorigenesis in Trp53 mutant mice. Nat Genet 36, 63–68.
Liu Y, Colosimo AL, Yang XJ, Liao D (2000). Adenovirus E1B 55-kilodalton oncoprotein inhibits p53 acetylation by PCAF. Mol Cell Biol 20, 5540–5553.
Mahajan R, Delphin C, Guan T, Gerace L, Melchior F (1997). A small ubiquitin-related polypeptide involved in targeting RanGAP1 to nuclear pore complex protein RanBP2. Cell 88, 97–107.
Makhnevych T *et al*. (2009). Global map of SUMO function revealed by protein-protein interaction and genetic networks. Mol Cell 33, 124–135.
Mateu MG, Fersht AR (1998). Nine hydrophobic side chains are key determinants of the thermodynamic stability and oligomerization status of tumour suppressor p53 tetramerization domain. EMBO J 17, 2748–2758.
Matunis MJ, Coutavas E, Blobel G (1996). A novel ubiquitin-like modification modulates the partitioning of the Ran-GTPase-activating protein RanGAP1 between the cytosol and the nuclear pore complex. J Cell Biol 135, 1457–1470.
Matunis MJ, Wu J, Blobel G (1998). SUMO-1 modification and its role in targeting the Ran GTPase-activating protein, RanGAP1, to the nuclear pore complex. J Cell Biol 140, 499–509.
Monecke T, Guttler T, Neumann P, Dickmanns A, Gorlich D, Ficner R (2009). Crystal structure of the nuclear export receptor CRM1 in complex with Snurportin1 and RanGTP. Science 324, 1087–1091.
Monecke T *et al*. (2013). Structural basis for cooperativity of CRM1 export complex formation. Proc Natl Acad Sci USA 110, 960–965.
Muscolini M *et al*. (2009). Characterization of a new cancer-associated mutant of p53 with a missense mutation (K351N) in the tetramerization domain. Cell Cycle 8, 3396–3405.
Muscolini M, Montagni E, Palermo V, Di Agostino S, Gu W, Abdelmoula-Souissi S, Mazzoni C, Blandino G, Tuosto L (2011). The cancer-associated K351N mutation affects the ubiquitination and the translocation to mitochondria of p53 protein. J Biol Chem 286, 39693–39702.
Paraskeva E, Izaurralde E, Bischoff FR, Huber J, Kutay U, Hartmann E, Luhrmann R, Gorlich D (1999). CRM1-mediated recycling of snurportin 1 to the cytoplasm. J Cell Biol 145, 255–264.
Petosa C, Schoehn G, Askjaer P, Bauer U, Moulin M, Steuerwald U, Soler-Lopez M, Baudin F, Mattaj IW, Muller CW (2004). Architecture of CRM1/exportin1 suggests how cooperativity is achieved during formation of a nuclear export complex. Mol Cell 16, 761–775.
Reverter D, Lima CD (2005). Insights into E3 ligase activity revealed by a SUMO-RanGAP1-Ubc9-Nup358 complex. Nature 435, 687–692.
Rodriguez MS, Desterro JM, Lain S, Midgley CA, Lane DP, Hay RT (1999). SUMO-1 modification activates the transcriptional response of p53. EMBO J 18, 6455–6461.
Saitoh H, Pu R, Cavenagh M, Dasso M (1997). RanBP2 associates with Ubc9p and a modified form of RanGAP1. Proc Natl Acad Sci USA 94, 3736–3741.
Santiago A, Godsey AC, Hossain J, Zhao LY, Liao D (2009). Identification of two independent SUMO-interacting motifs in Daxx: evolutionary conservation from *Drosophila* to humans and their biochemical functions. Cell Cycle 8, 76–87.
Sekiyama N, Ikegami T, Yamane T, Ikeguchi M, Uchimura Y, Baba D, Ariyoshi M, Tochio H, Saitoh H, Shirakawa M (2008). Structure of the small ubiquitin-like modifier (SUMO)-interacting motif of MBD1-containing chromatin-associated factor 1 bound to SUMO-3. J Biol Chem 283, 35966–35975.
Song J, Durrin LK, Wilkinson TA, Krontiris TG, Chen Y (2004). Identification of a SUMO-binding motif that recognizes SUMO-modified proteins. Proc Natl Acad Sci USA 101, 14373–14378.
Song J, Zhang Z, Hu W, Chen Y (2005). Small ubiquitin-like modifier (SUMO) recognition of a SUMO binding motif: a reversal of the bound orientation. J Biol Chem 280, 40122–40129.
Stindt MH, Carter S, Vigneron AM, Ryan KM, Vousden KH (2011). MDM2 promotes SUMO-2/3 modification of p53 to modulate transcriptional activity. Cell Cycle 10, 3176–3188.
Stommel JM, Marchenko ND, Jimenez GS, Moll UM, Hope TJ, Wahl GM (1999). A leucine-rich nuclear export signal in the p53 tetramerization domain: regulation of subcellular localization and p53 activity by NES masking. EMBO J 18, 1660–1672.
Ullmann R, Chien CD, Avantaggiati ML, Muller S (2012). An acetylation switch regulates SUMO-dependent protein interaction networks. Mol Cell 46, 759–770.
Waterman JL, Shenk JL, Halazonetis TD (1995). The dihedral symmetry of the p53 tetramerization domain mandates a conformational switch upon DNA binding. EMBO J 14, 512–519.
Wen W, Meinkoth JL, Tsien RY, Taylor SS (1995). Identification of a signal for rapid export of proteins from the nucleus. Cell 82, 463–473.
Werner A, Flotho A, Melchior F (2012). The RanBP2/RanGAP1*SUMO1/Ubc9 complex is a multisubunit SUMO E3 ligase. Mol Cell 46, 287–298.
Wong KB, DeDecker BS, Freund SM, Proctor MR, Bycroft M, Fersht AR (1999). Hot-spot mutants of p53 core domain evince characteristic local structural changes. Proc Natl Acad Sci USA 96, 8438–8442.
Wu SY, Chiang CM (2009). Crosstalk between sumoylation and acetylation regulates p53-dependent chromatin transcription and DNA binding. EMBO J 28, 1246–1259.
Zhang XD, Goeres J, Zhang H, Yen TJ, Porter AC, Matunis MJ (2008). SUMO-2/3 modification and binding regulate the association of CENP-E with kinetochores and progression through mitosis. Mol Cell 29, 729–741.
Zhang Y, Xiong Y (2001). A p53 amino-terminal nuclear export signal inhibited by DNA damage-induced phosphorylation. Science 292, 1910–1915.
Zhao LY, Santiago A, Liu J, Liao D (2007). Repression of p53-mediated transcription by adenovirus E1B 55-kDa does not require corepressor mSin3A and histone deacetylases. J Biol Chem 282, 7001–7010.
Zhu S, Zhang H, Matunis MJ (2006). SUMO modification through rapamycin-mediated heterodimerization reveals a dual role for Ubc9 in targeting RanGAP1 to nuclear pore complexes. Exp Cell Res 312, 1042–1049.